Supplementary information

Supplementary discussion:

Critical radius for surface-tension assisted conformal coating

Surface-tension assisted conformal coating is realized by reducing the surface energy at the liquid-air interface at the cost of increasing the elastic energy when the coating material is deformed. We analytically model the surface tension during NEC device coating by considering an elastic sheet of thickness h, in loose contact with a rigid cylinder of radius R (Fig. 2k). Both the sheet and cylinder are wetted with the same liquid. The sheet deformation reduces the liquid-air area A and therefore the surface energy γA (γ being the surface tension) at the cost of increasing the elastic energy. At the critical radius R_C, the increase of elastic energy $dE_{el} = B/R_C^2 dx$ equals the decrease of surface energy $2\gamma cos\alpha dx$, where α is the contact angle of the liquid on the surface[1] which we set to zero

$$R_C = \sqrt{\frac{B}{2\gamma}} \qquad \text{(Eq. S1)},$$

where B is the bending modulus, a geometry and material related property describing the resistance of an elastic sheet against bending deformation[2], which dictates its ability to comply with a curved surface. B is determined by[3]

$$B = \frac{Eh^3}{12(1-\nu^2)} \qquad \text{(Eq. S2)},$$

where *E* is the Young's modulus of the elastic material, *h* is the thickness of the elastic sheet, and *v* is Poisson ratio of the material.

Combining Eq. S1 and Eq. S2, we obtain:

$$R_C = \sqrt{\frac{B}{2\gamma}} = \sqrt{\frac{Eh^3}{24\gamma(1-\nu^2)}} \qquad \text{(Eq. S3)}$$

For NEC devices which is mainly composed of SU-8, We use $E_{SU-8} = 2.02\ GPa$ and $\nu_{SU-8} = 0.22$, and $\gamma = 71.97\ \mathrm{mN/m}$ for distilled water, we obtain the critical dimeter $d_C = 2R_C$ at h = 0.5 μm and 1 μm to be 24.7 μm and 70.1 μm respectively. The $d_C - h$ relation is plotted as the boundary between two regimes in Fig. 2l, in which for any h, the probes with diameters larger than d_C are in the "attach" regime. For $h \leq 1$ μm, this "attach" regime covers most conventional brain probes. For instance, optical fibers used in optogenetics studies typically have diameters larger than 200 μm, which can be coated by all NEC devices demonstrated in the study. In other applications, fibers and glass pipettes may be sharpened with tip diameter around 20 μm[4], in which case the NEC devices with $h = 0.5$ μm will form conformal attachment.

We note that $B \propto h^3$. As we reduced h by at least 10 fold from most previously reported flexible probes[5-7], we reduced B by at least 10^3 times. The unconventional thickness and flexibility of NEC devices is the key to facile coating on micro-scale surfaces.

We note that a prerequisite of the above model is that both objects are completely wetted by the liquid to maximize the reduction in the surface energy[8,9], e.g. the contact angle of the liquid on the surface $\alpha = 0$. To make the surfaces of both NEC devices and target probes hydrophilic, we treated them with oxygen plasma before releasing[10], which significantly increased their surface energy and achieved contact angle $\alpha < 5^{\circ}$ as shown in Fig. 2k.

Supplementary figures

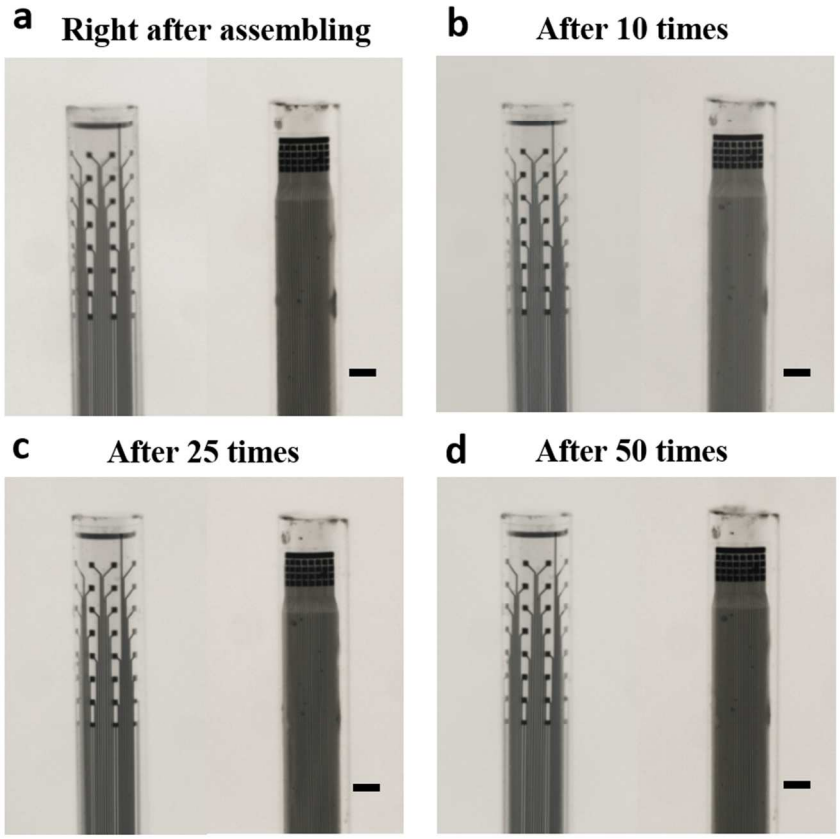

SFig. 1: In-vitro test of NEC devices adhesion. Photographs of two multifunctional probes at immediately after assembling (**a**), and after 10 times (**b**), 25 times (**c**) and 50 times (**d**) insertion-extraction cycles in agarose gel (0.5%), showing that the NEC device remained conformal coating on the host probe after extensive insertion tests. Scale bar: 100 μm.

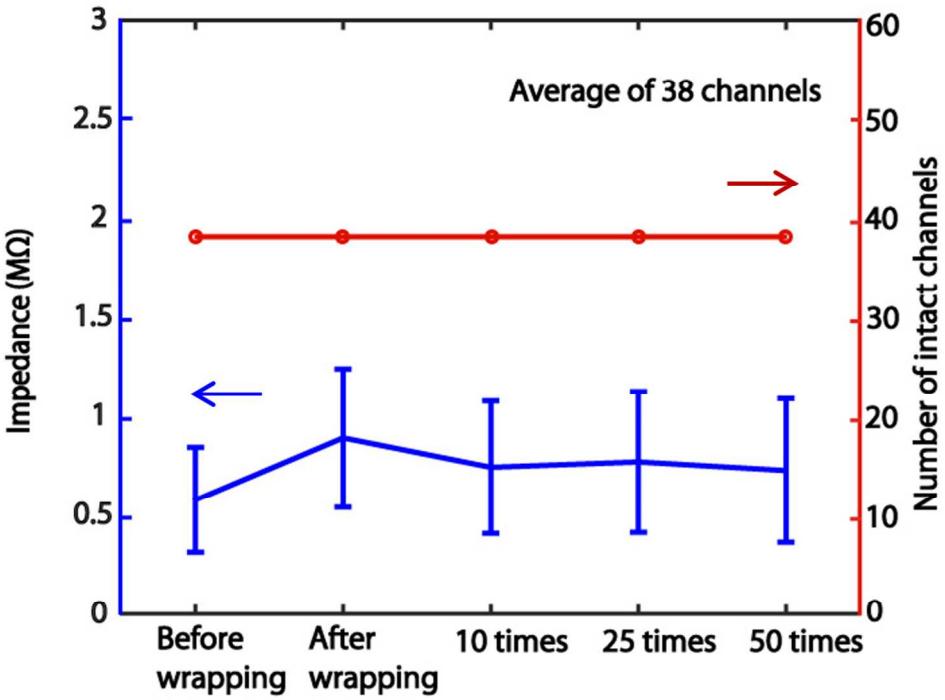

SFig. 2: Averaged impedance of 38 electrodes on NEC devices in PBS before wrapping, after wrapping, and after 10, 25 and 50 insertion-extraction cycles in agarose gel, showing the mechanical and electrical integrity of the NEC devices after extensive handling. Error bars show the standard deviation of impedance among 38 electrodes. The number of active channels (red) also remains the same through the test.

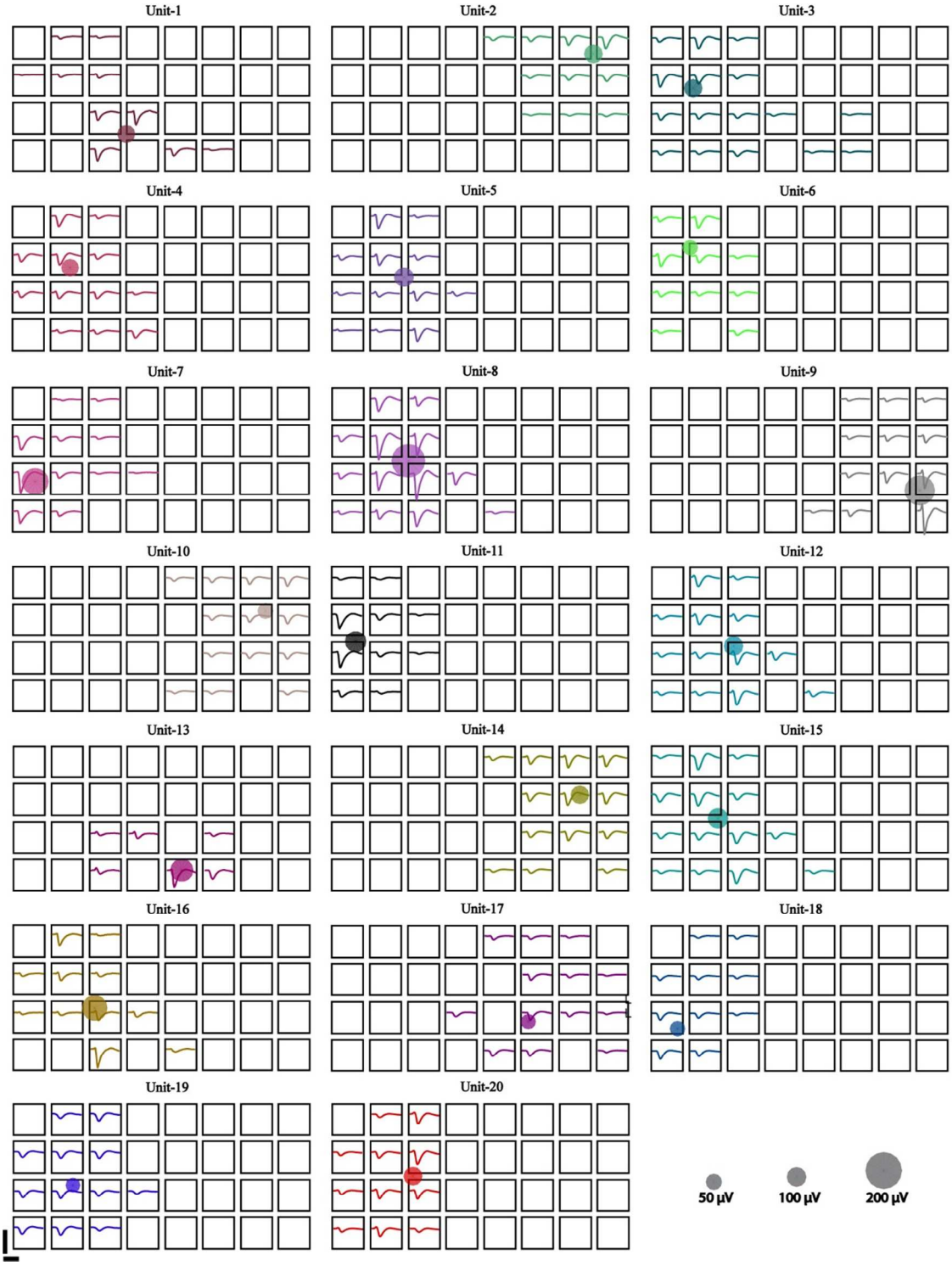
Unit-1
Unit-2
Unit-3
Unit-4
Unit-5
Unit-6
Unit-7
Unit-8
Unit-9
Unit-10
Unit-11
Unit-12
Unit-13
Unit-14
Unit-15
Unit-16
Unit-17
Unit-18
Unit-19
Unit-20
50 µV
100 µV
200 µV

SFig. 3: Waveforms of Individual units (a total of 20) plotted on the recording electrodes, using the same color code as in Fig. 3c. Waveforms were averaged from all events recorded in 12 mins. Scale bar: 100 μV (vertical) and 1 ms (horizontal). Dots show the location of neurons inferred from triangulation where the size of the dots was scaled to the largest peak amplitude in waveforms of the corresponding unit. Same color code and amplitude scale as in Fig. 3c

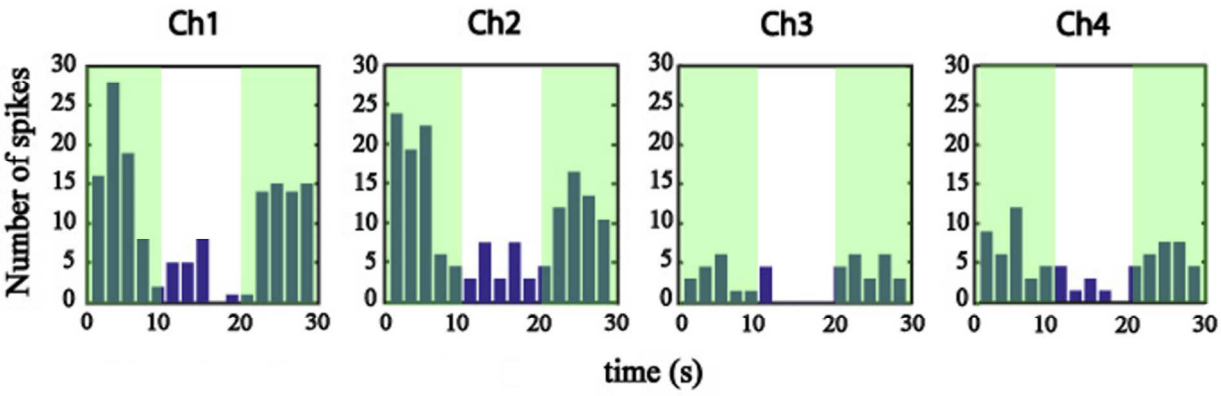

SFig. 4: Histogram showing the firing rate change of individual channels shown in Fig 4b in response of optical stimuli. Shades mark the presence of laser stimulation.

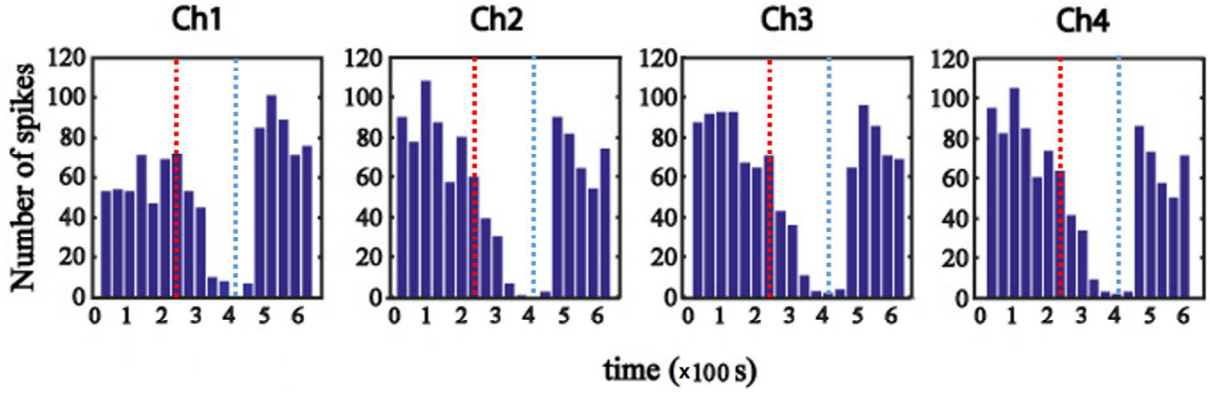

SFig. 5: Histogram showing the firing rate change of individual channels shown in Fig 4e in response of controlled drug infusion. Dashed lines mark the start and finish of the CNQX infusion.

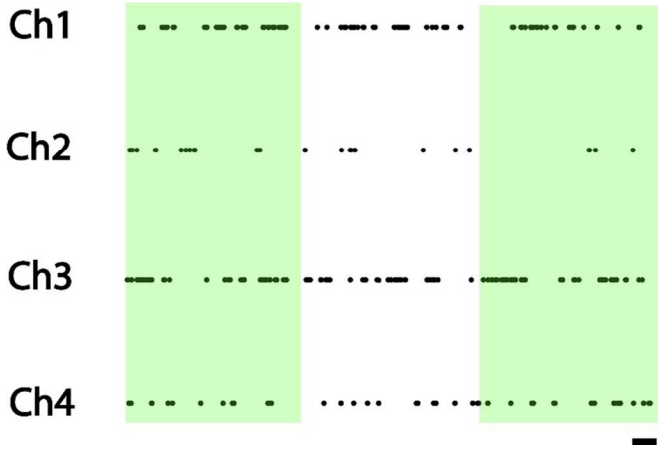

SFig. 6: Control experiment at **532 nm Laser excitation** on transgenic optogentic mouse (Thy1-mhChR2-EYFP), showing little evoked neural activity. Shade marks the presence of optical stimulation at 532 nm. Dots indicate the occurrence of APs. Average firing rate ratio per second at laser on and off: 1.17 ± 0.21. (t test with p=0.33). Horizontal bar: 2 s.

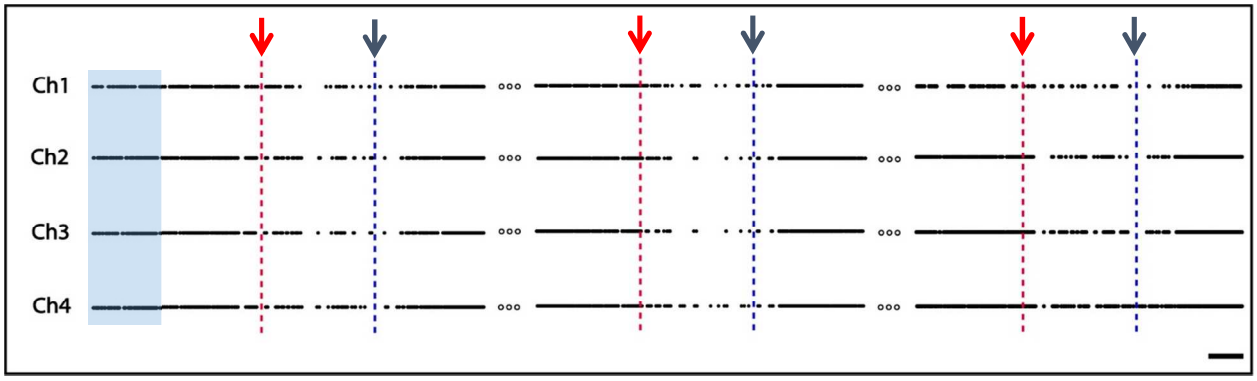

SFig. 7: **Multiple repetitions of controlled drug infusion.** Example recording from 4 channels implanted in a wild-type mouse in mPFC cortex showing consistent inhibition effect for every repetition. Arrows mark the start and finish of the controlled infusion of CNQX at 50 nl/s. Dots mark the occurrence of APs. Shade marks the presence of PBS infusion at 50 nl/s. Scale bar: 1 min.

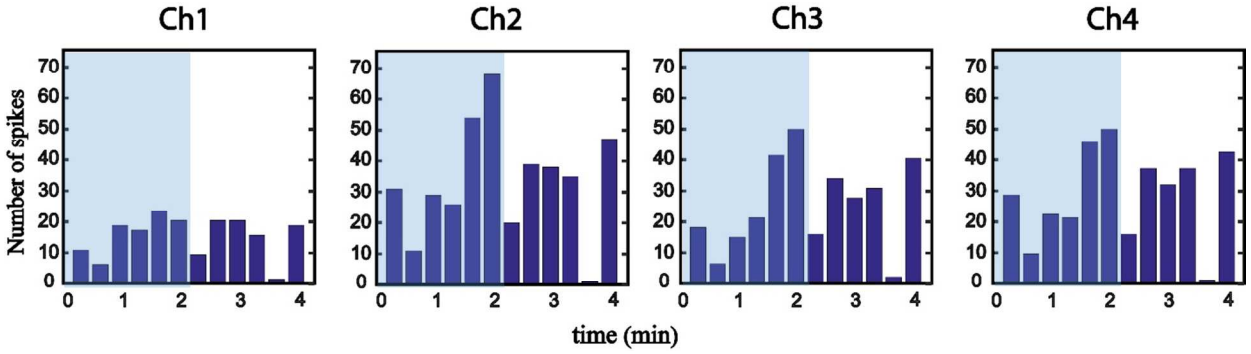

SFig. 8: Histogram showing little firing rate change of individual channels in response of 1xPBS injection. Shade marks the presence of PBS infusion at 50 nl/s. To exclude the latency effect of drug (60 s for CNQX injection), 120 s recording after PBS infusion is shown.

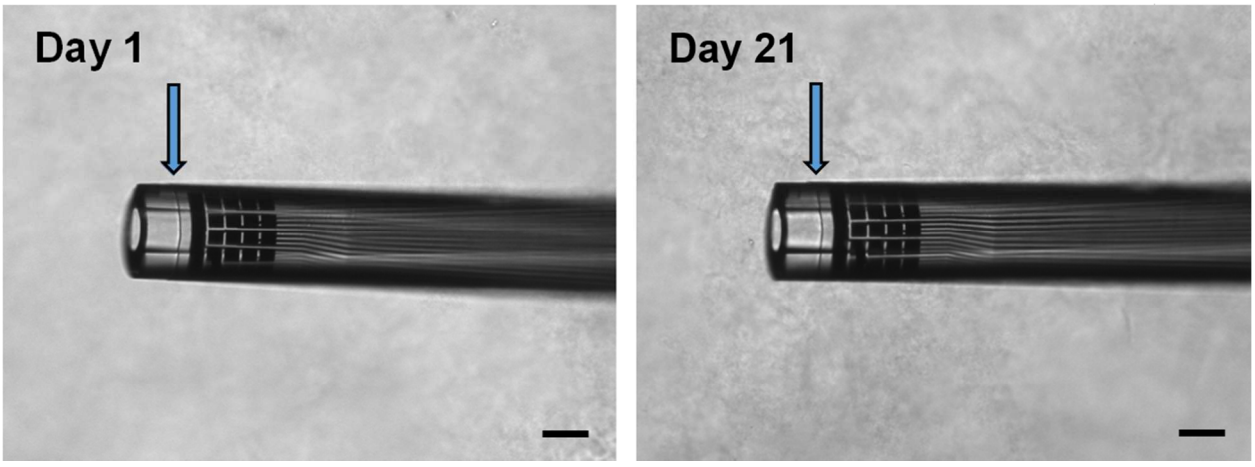

SFig. 9: **Three-week in vitro test.** Photographs of the same multifunctional probe immediately after inserting into agarose gel (left: Day 1) and after three week (right: Day 21), showing that the NEC device remained conformal coating on the host probe. Scale bar: 100 μm.

1. Py, C.; Reverdy, P.; Doppler, L.; Bico, J.; Roman, B.; Baroud, C. N. *Phys. Rev. Lett.* **2007,** 98, (15).
2. Steif, P. S., *Mechanics of materials*. Pearson Education, Inc.: Upper Saddle River, New Jersey, 2012.
3. Landau, L. D.; Lifshi͡ts, E. M.; Kosevich, A. d. M.; Pitaevskiĭ, L. P., *Theory of elasticity*. 3rd English ed.; Pergamon Press: Oxford Oxfordshire ; New York, 1986; p viii, 187 p.
4. Canales, A.; Jia, X.; Froriep, U. P.; Koppes, R. A.; Tringides, C. M.; Selvidge, J.; Lu, C.; Hou, C.; Wei, L.; Fink, Y.; Anikeeva, P. *Nat. Biotechnol.* **2015,** 33, (3), 277-84.
5. Kim, T. I.; McCall, J. G.; Jung, Y. H.; Huang, X.; Siuda, E. R.; Li, Y.; Song, J.; Song, Y. M.; Pao, H. A.; Kim, R. H.; Lu, C.; Lee, S. D.; Song, I. S.; Shin, G.; Al-Hasani, R.; Kim, S.; Tan, M. P.; Huang, Y.; Omenetto, F. G.; Rogers, J. A.; Bruchas, M. R. *Science* **2013,** 340, (6129), 211-6.
6. Seymour, J. P.; Kipke, D. R. *Biomaterials* **2007,** 28, (25), 3594-607.
7. Jeong, J. W.; McCall, J. G.; Shin, G.; Zhang, Y. H.; Al-Hasani, R.; Kim, M.; Li, S.; Sim, J. Y.; Jang, K. I.; Shi, Y.; Hong, D. Y.; Liu, Y. H.; Schmitz, G. P.; Xia, L.; He, Z. B.; Gamble, P.; Ray, W. Z.; Huang, Y. G.; Bruchas, M. R.; Rogers, J. A. *Cell* **2015,** 162, (3), 662-674.
8. Lester, G. R. *Nature* **1966,** 209, 1126.
9. Lester, G. R. *J. Colloid. Sci.* ***1961,*** *16, 315.*
10. Walther, F., Drobek, T., Gigler, A. M., Hennemeyer, M., Kaiser, M., Herberg, H., Shimitsu, T., Morfill, G. E. and Stark, R. W. **2010,** *Surf. Interface Anal. 42, 1735-1744.*

Smovie 1.

Video shows the real-time firing sequence of the sorted units at their estimated position relative to the 2D electrode array. The firing neurons were highlighted for every event. Recording time: 20 s.